

IoT-LLM: Enhancing Real-World IoT Task Reasoning with Large Language Models

Tuo An^{1,2*}, Yunjiao Zhou¹, Han Zou¹, Jianfei Yang¹.

¹Nanyang Technological University ²Nanjing University

Abstract

Large Language Models (LLMs) excel in textual and visual tasks but often produce outputs that defy physical laws when dealing with physical-world reasoning tasks. Inspired by human cognition—where perception is fundamental to reasoning—we explore augmenting LLMs with enhanced perception abilities using Internet of Things (IoT) sensor data and pertinent knowledge for IoT-sensory task reasoning in the physical world. In this work, we systematically study LLMs’ capability to address real-world IoT-sensory tasks by augmenting their perception and knowledge base, and then propose a unified framework, IoT-LLM, to enhance such capability. In IoT-LLM, we customize three steps for LLMs: preprocessing IoT data into formats amenable to LLMs, expanding their understanding via IoT-oriented retrieval-augmented generation based on in-context learning and activating their commonsense knowledge through chain-of-thought prompting and specialized role definitions. We design a new benchmark comprising five real-world tasks with varying data types and reasoning complexities to evaluate the performance of IoT-LLM. Experimental results on six LLMs reveal that IoT-LLM significantly improves the performance of IoT-sensory task reasoning of LLMs, with models like GPT-4o-mini showing a 49.4% average improvement over previous methods.

1 Introduction

Recent advancements in large generative models have showcased their exceptional performance and versatility in handling complex tasks across textual and visual domains, as evidenced by the GPT series (Radford et al., 2018, 2019; Brown et al., 2020; Achiam et al., 2023; OpenAI, 2023) and visual generation models (Dosovitskiy et al., 2020; Liu

et al., 2021; Ho et al., 2020; Peebles and Xie, 2023; Blattmann et al., 2023). However, these models could occasionally generate outputs that are physically implausible, often referred to as “hallucinations” (Alkaissi and McFarlane, 2023; Huang et al., 2023). Even advanced video generation models, e.g., Sora (Brooks et al., 2024), are susceptible to producing animations that contravene fundamental physical laws, such as a video clip containing a tipping water glass that appears to defy gravity. These observations suggest that generative models may not really comprehend and apply physical laws of the physical world as accurately as humans when acting as world simulators. This has renewed interest in research on the *World Model* that focuses on understanding and modeling the physical world in a brain-like manner (Dawid and LeCun, 2023; Garrido et al., 2024; Liu et al., 2024).

Unlike LLMs that map descriptions of the physical world to a latent space and perform reasoning by predicting the text sequence according to the probability, research on human cognitive science illustrates a different mechanism. The human brain comprises multiple mutually-functional areas, of which the important components include the temporal and occipital lobes for perception, and the frontal cortex for reasoning (Churchland and Sejnowski, 1988; Saxe et al., 2009; Hobeika et al., 2016; Grèzes et al., 2001). Notably, perception is the primary mechanism through which information about the physical world is acquired, and then effective reasoning is inherently dependent on accurate perception. However, in LLMs, the physical world is only “perceived” through natural language, i.e., concepts and words in the semantic space, which denotes an indirect representation and abstraction of the physical world. A recent study in Nature shows language is primarily a tool for communication rather than thought (Fedorenko et al., 2024), so reasoning the physical-world problem with only language is limited. To enable LLMs with better

*This work was conducted during the author’s research internship at MARS Lab, NTU.

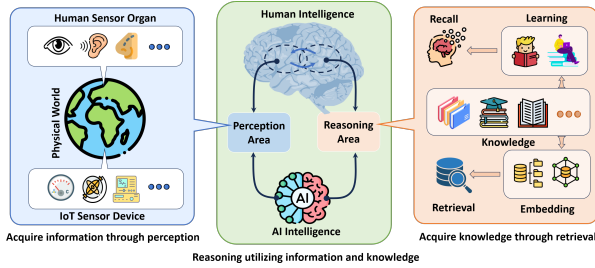


Figure 1: Inspired by human cognitive science, we augment LLMs with physical world perception from IoT data. Furthermore, by retrieving pertinent knowledge about IoT tasks, we enhance the reasoning capabilities of LLMs in executing real-world applications.

reasoning capability in the real world, perception is highly demanded. Recent research on Vision Language Models (VLMs) builds the connection between visual perception and languages (Zhang et al., 2024a), yet the vision is only one of the various perceptual modalities. Many aspects of the physical world are still not perceived by existing LLMs.

We draw inspiration from human cognition, which integrates perception and reasoning with domain knowledge. Humans perceive the world through sensory organs (e.g., eyes and ears), while IoT sensors serve as analogous "sensory organs" for machines, capturing physical-world data for automation. Since the first IoT sensor was introduced in the 1980s to monitor Coke machine inventories (Madakam et al., 2015), these sensors have become essential for modeling the physical environment. Humans further process perception data using domain knowledge acquired through experience and education. Similarly, large language models (LLMs) can leverage in-context learning to integrate domain knowledge about the physical world and IoT sensors, enhancing their reasoning capabilities. As illustrated in Fig. 1, we hypothesize that combining IoT-enabled perception data with relevant knowledge can enable LLMs to tackle complex real-world tasks. In this work, we aim to explore three key questions: (1) What types of real-world tasks can LLMs perform using IoT-enabled perception? (2) How can LLM capabilities be further enhanced for such tasks? (3) Do LLMs truly comprehend perception data and apply knowledge effectively to solve real-world problems?

Previous studies have primarily shown the viability of using LLMs for IoT-sensory task reasoning (Xu et al., 2024a; Ji et al., 2024), but we find

that these studies are not carefully scrutinized. (1) These studies only focus on specific tasks, such as R-peak identification and action recognition. The choices of tasks are not comprehensive, thus lacking a benchmark to evaluate the performance of the methods. (2) They directly input raw IoT data into LLMs for reasoning, but LLMs are not good at dense numerical data and calculation (Zhou et al., 2024; Gruver et al., 2024). (3) They only evaluate their effectiveness on closed-source LLMs, and lack a comprehensive study of benchmarking open-source LLMs with different parameter size. (4) While some of them also incorporate external domain knowledge to aid LLMs in task handling, they rely on expert-designed knowledge, which is costly, time-consuming, and challenging to adapt to new tasks due to the need for bespoke expert input.

To bridge this gap and address the proposed questions, we conduct a comprehensive study on leveraging LLMs for various IoT tasks in the physical world. First, we evaluate LLMs' ability to handle IoT classification and regression challenges by introducing a new benchmark comprising five representative IoT sensory tasks: human activity recognition, industrial anomaly detection, heartbeat anomaly detection, WiFi-based human sensing, and indoor localization. These tasks span diverse domains, including daily life, industrial applications, and healthcare, with varying levels of complexity and difficulty. Next, we propose IoT-LLM, a unified framework to enhance LLMs' reasoning capabilities with IoT data. IoT-LLM includes three key components: IoT data simplification and enrichment, IoT-oriented knowledge retrieval augmentation, and prompt configuration. Finally, we assess LLMs' comprehension and problem-solving abilities by analyzing their generated reasoning processes. Results demonstrate that IoT-LLM enables LLMs to perform more precise and domain-specific analyses compared to baseline methods, achieving expert-level insights across IoT tasks.

In summary, our contributions are as follows:

- We systematically study how LLMs can address real-world problems by perceiving the physical world via IoT sensor data.
- We propose a unified framework to address IoT-related real-world problems, which enhances the capability of LLMs through three tailored steps. To the best of our knowledge,

this is the first unified framework for IoT-sensory tasks in the physical world.

- We establish the first benchmark for IoT-sensory task reasoning, including five real-world tasks with various types of IoT data. Empirical results show that our IoT-LLM significantly improves the performances of all base LLMs on IoT-sensory tasks.

2 Related work

Existing literature on LLMs in IoT mainly regards LLM as a user interface or as coordinators in smart machines (Li et al., 2023; Cui et al., 2023; Du et al., 2023). However, in these studies, LLMs function as intermediaries and do not directly interpret IoT data to perform real-world tasks. Recent studies, such as Penetrative AI (Xu et al., 2024b) and HarGPT (Ji et al., 2024), have begun integrating IoT data into LLMs for specific tasks, leveraging their inherent knowledge bases. Despite these advancements, the exploration of LLMs processing IoT data remains nascent. Penetrative AI converts IoT data into textual and numerical formats for basic tasks like R-peak identification in ECG data, heavily relying on manually crafted expert knowledge, which limits automation and scalability. Similarly, HarGPT processes raw IMU data to recognize human activities using a chain of thought technique but is restricted to this specific data type and task, not demonstrating the broader applicability of LLMs. While these studies offer initial insights into using LLMs in the IoT domain, they lack a comprehensive framework to fully leverage LLM capabilities or systematically benchmark current LLMs on IoT sensory tasks, which is the primary focus of our research.

3 Methodology

In this section, we define the problem for IoT-sensory task reasoning with LLM and introduce our research methodology. The formulated research problem is how to leverage LLM and in-context learning for task reasoning for IoT data, termed as *IoT-sensory task reasoning*, e.g., using accelerators data for activity recognition or machine sensor for anomaly detection. The prompt for LLM should include two parts: data, as a way to perceive the physical world, and the task description, such as “Is it a Normal heartbeat (N) or Premature ventricular contraction beat (V)?”, serves as the query. To evaluate

the performance of the task, we build a new benchmark including 5 real-world tasks with different IoT data types and difficulty levels, encompassing both classification and regression problems.

At first, we employ LLMs to execute IoT-sensory tasks in a basic setting, similar to Penetrative AI (Xu et al., 2024a), where the prompt provided to the LLMs includes raw IoT data, the associated query and optionally, specially designed expert knowledge. However, the performance of LLMs remains suboptimal. As shown by the baseline results in Table 2, even GPT-4o-mini only achieves an accuracy of 37.3% for 3-way activity recognition and 44% for heartbeat anomaly detection based on this approach. These preliminary results akin to near-random guessing suggest a lack of comprehension of IoT data and tasks by this naive prompting way. Upon analyzing the characteristics of IoT data and real-world tasks, we identify that the challenges stem from the abstraction of dense numeric data and the lack of domain knowledge within LLMs. To address these challenges, we propose a unified framework (Fig. 2) consisting of three key stages: (1) IoT data simplification and enrichment, (2) IoT-oriented knowledge augmentation, and (3) prompt configuration. Each stage addresses specific difficulties encountered by LLMs for IoT-sensory task reasoning, and we introduce each stage one by one.

3.1 IoT data simplification and enrichment

Unlike textual human tasks that have been learned by LLMs, IoT data for IoT-sensory task reasoning presents unique challenges that hinder LLMs’ comprehension. Firstly, IoT data encompasses a diverse range of types and forms, many of which are complex time-series data (e.g., electrocardiogram readings) (Goldberger et al., 2000) or multi-variant data (e.g., WiFi CSI) (Yang et al., 2024). LLMs often struggle with accurately interpreting dense numerical data, especially when it involves long-sequence time-series data (Zhang et al., 2024b). Secondly, IoT data is typically composed of raw numerical values. This data often lacks essential textual annotations, such as units of measurement and metadata about the data collection process, which are critical for LLMs to interpret effectively in real-world applications. In summary, raw IoT data requires (1) appropriate simplification and (2) information enrichment. Previous studies (Xu et al., 2024a; Ji et al., 2024) have employed down-sampling techniques for time-series data but they only achieve coarse-grained simplification at a length level with-

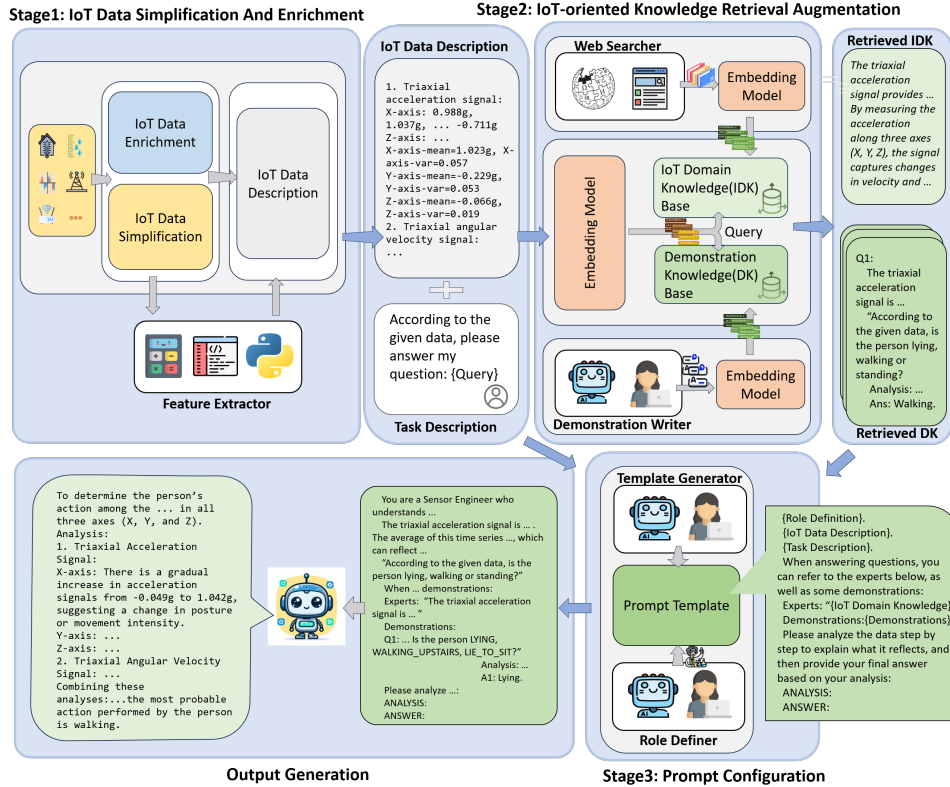


Figure 2: In our framework, IoT data is initially preprocessed to create a data description. Next, relevant IoT domain knowledge and task-specific demonstrations are retrieved. These elements are then combined into a prompt, which is input into a LLM to generate the final output.

out enhancing the informational content of the IoT data. In contrast, we not only simplify IoT data at the token level but also enrich the IoT data by providing additional information to facilitate better understanding by LLMs. In this way, we transform complex raw IoT data into an LLM-friendly format for IoT-sensory task reasoning (as illustrated in Fig. 6 in Appendix D).

IoT data simplification. To achieve effective simplification, it is crucial to understand why LLMs struggle with dense numeric data. Firstly, according to recent research (Gruber et al., 2024; Spathis and Kawsar, 2023), tokenization methods, such as Byte Pair Encoding (BPE) often fragment numbers into tokens that do not align with their digits, resulting in inconsistent tokenization of floating-point numbers and complicating arithmetic operations. Therefore, in addition to down-sampling and keeping fixed precision (e.g., two digits of precision) to efficiently manage context length, we propose to insert spaces between digits to ensure distinct tokenization of each digit and use a comma (“,”) to separate each time step in a time series. Sec-

ondly, the complexity of long-sequence IoT data poses significant challenges for LLMs in analysis. To assist LLMs in processing this data, we extract essential statistical features, e.g., mean, variance, and FFT mean, utilizing external tools, such as Python scripts. We find that these fundamental features are strong enough for reasoning in classic IoT-sensory tasks. By doing so, we not only simplify IoT data at both length and token levels but also transform it into a format that is more suitable for tokenization and processing by LLMs.

IoT data enrichment. As previously noted, IoT data alone is insufficient for LLMs to effectively perform real-world tasks. To address this, we enrich the data by incorporating contextual information about the physical world. Specifically, we provide a comprehensive overview of IoT data collection and the integration of physical information. For instance, in human activity recognition (HAR) tasks using inertial measurement unit (IMU) data, including triaxial acceleration and angular velocity from accelerometers and gyroscopes, we detail the data collection process by specifying metadata

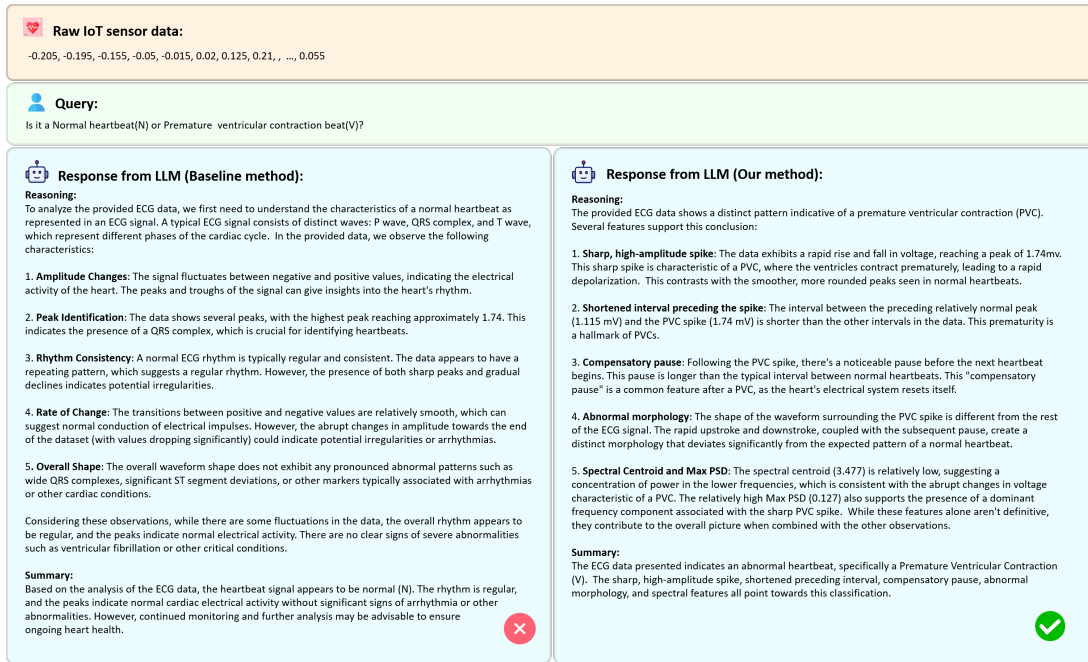


Figure 3: **Response examples comparing the baseline method and our approach in heartbeat anomaly detection.** The baseline method offers logically coherent but generalized analyses, whereas our method provides deeper insights and more precise descriptions of ventricular premature contraction characteristics, resulting in more professional and accurate responses.

such as sampling frequency (e.g., 10 Hz), device placement, and measurement units (e.g., gravitational acceleration and radians per second). This method allows LLMs to align the three-axis IMU data with the body's spatial orientations and grasp the physical significance of these values, thereby improving their understanding of the task in the physical world.

3.2 IoT-oriented Knowledge Retrieval Augmentation

In IoT-sensory task reasoning, the knowledge of LLMs to perform tasks is significant. For example, detecting abnormal heartbeats from electrocardiogram (ECG) data requires interpreting ECG signals and associating them with specific heartbeat states (e.g., premature ventricular contraction), necessitating specialized domain knowledge. Although previous research (Xu et al., 2024a) proposes to include specific expert knowledge for specific tasks, the augmentation is task-specific and added manually, which is time-consuming and not scalable. To address this, we enable LLMs with IoT knowledge in an automatic fashion. Inspired by the in-context learning capability of LLMs, we also retrieve task-specific demonstrations, such as question-answer pairs, to guide LLMs in effectively utilizing IoT

data for analyzing IoT-sensory tasks.

We begin by constructing an IoT domain knowledge base and a demonstration knowledge base for retrieving domain knowledge and task-specific demonstrations. Next, we utilize an embedding model to convert texts into vectors, storing these as key-value pairs for efficient search capabilities. Metadata is also stored alongside the embeddings to enhance retrieval quality through advanced techniques like metadata filtering. We then retrieve relevant knowledge using a hybrid search method that combines keyword-based and embedding-based retrievers to ensure the retrieval of context-rich information. Finally, a re-ranking technique is applied to refine the similarity between queries and retrieved texts, filtering out the top-m most relevant pieces to obtain pertinent knowledge. Further details of this procedure are provided in Appendix A.

Seamless expansion to new tasks. By employing this automatic retrieval method to acquire relevant knowledge, as opposed to the manual design of expert knowledge utilized in (Xu et al., 2024a), our approach allows for seamless expansion to address new tasks. This is achieved simply by adding additional documents pertinent to the new task into the IoT knowledge base, while the rest of the framework's pipeline remains unchanged. In the real

world, it’s not possible to tailor the prompt for thousands of IoT tasks, highlighting our advantages.

3.3 Prompt Configuration

In addition to augmenting LLMs’ knowledge by providing external documents in the context utilizing the in-context learning capability of LLMs, we further invoke LLMs’ internal knowledge by carefully configuring the prompt. Recent research highlights LLMs’ robust role-playing abilities (Park et al., 2023). We exploit this by assigning specific roles to LLMs for particular tasks. For example, we have LLMs adopt the role of a professional doctor for heartbeat anomaly detection, thereby utilizing their internal domain knowledge. Furthermore, since LLMs’ reasoning capabilities can be significantly improved by decomposing problems into smaller parts (Wei et al., 2022), we divide the reasoning process into two steps: first prompting LLMs to analyze IoT data and tasks, and then providing the final answer based on this analysis. This approach also allows us to assess the LLMs’ understanding of IoT data and their ability to perform IoT tasks through the generated analysis. Finally, we use a prompt template (see Fig. 4 in Appendix D) to structure the content discussed. The final prompt is crafted based on the template and then input into a downstream LLM, which produces the final output, including both analysis and the answer to the specified task.

4 Experiments

4.1 IoT Reasoning Benchmark

IoT Sensory Tasks. To comprehensively assess the capability boundaries of LLMs for IoT-sensory task reasoning, we develop a new benchmark comprising five real-world tasks with diverse IoT data types and difficulty levels: (1) Human Activity Recognition (HAR) using Inertial Measurement Unit (IMU) data, (2) Industrial anomaly detection using metrics such as temperature, cooling power, and cooling efficiency, (3) Heartbeat anomaly detection using Electrocardiogram (ECG) data, (4) Human sensing using WiFi Channel State Information (CSI), and (5) Indoor localization based on WiFi signal strength.

IoT datasets. In our benchmark, we select publicly available IoT datasets for five tasks to ensure fairness. Specifically, for Human Activity Recognition, we use the Smartphone-Based Recognition of Human Activities and Postural Transi-

tions Dataset (Reyes-Ortiz et al., 2015). For Industrial Anomaly Detection, we use the Condition Monitoring of Hydraulic Systems Dataset (Helwig et al., 2018). For Heartbeat Anomaly Detection, we employ the MIT-BIH Arrhythmia Database (Goldberger et al., 2000). For the Human Sensing task, we utilize a dataset collected with a TP-Link TL-WDR4300 WiFirouter operating at 5 GHz with a 40 MHz bandwidth (Zhuravchak et al., 2022). For the Indoor Localization task, we use a dataset collected in a laboratory environment using an IoT system developed in (Huang et al., 2022). Due to the complexity of some datasets with numerous classes, we simplify them by using subsets, as done in previous studies (Ji et al., 2024). Further details on dataset usage are provided in Appendix B.

LLM Baselines. In the conducted experiments, we utilize a combination of proprietary and open-source LLMs, including GPT-3.5-turbo, GPT-4o-mini, claude-3.5-sonnet, gemini-pro, Mistral-7B¹, and LLaMA-2-7B². This diverse selection of models enables a comprehensive evaluation of the LLMs’ capabilities in executing IoT-sensory tasks and provides insights into their respective strengths and limitations in real-world applications.

4.2 Results and analysis

To evaluate the efficacy of our proposed framework in enhancing the capabilities of IoT-sensory task reasoning for LLMs, We employ Penetrative AI (Xu et al., 2024a) as baseline method, utilizing prompts that include raw IoT data, corresponding task descriptions, and optionally, specially designed expert knowledge. The overall performance of LLMs on IoT-sensory tasks is shown in Table 1 and Table 2. The results indicate that our proposed framework significantly enhances the performance of all the LLMs in completing IoT-sensory tasks in real-world scenarios. After analyzing the overall performance of LLMs in the task reasoning, we can answer the questions we proposed in the introduction now. Here is a summary of our arguments regarding the IoT-sensory task reasoning with LLMs.

LLMs excel in various IoT-sensory tasks but struggle with complex data challenge. Experimental results indicate that advanced LLMs, such

¹<https://huggingface.co/mistralai/Mistral-7B-Instruct-v0.3>

²<https://huggingface.co/togethercomputer/LLaMA-2-7B-32K>

Method		Model					
		Llama2-7B	Mistral-7B	Claude-3.5	Gemini-pro	GPT-3.5	GPT-4o-mini
Base-line	RMSE (m)	0.374	11.570	0.829	2.318	2.598	0.741
	MAE (m)	0.313	9.347	0.696	1.814	1.937	0.581
	STD	0.903	6.856	1.607	5.999	6.715	1.502
Ours	RMSE (m)	0.355	9.995	0.404	0.313	0.719	0.402
	MAE (m)	0.295	7.980	0.341	0.265	0.592	0.341
	STD	0.852	11.146	0.706	0.763	1.765	0.697
Improvement	RMSE (m)	+5.1%	+13.6%	+51.3%	+86.5%	+72.3%	+45.7%
	MAE (m)	+5.8%	+14.6%	+51.0%	+85.4%	+69.4%	+41.3%

Table 1: **Performance of LLMs on WiFi-based Indoor Localization task.** Since this is a regression task, we choose the Root Mean Square Error (RMSE), Mean Absolute Error (MAE), and standard deviation (STD) of the RMSE as the main performance metrics.

Model		IoT tasks (Accuracy \uparrow)				
		HAR-2cls	HAR-3cls	Heartbeat	Machine	Occupancy
Llama2-7B	Baseline	50.0%	32.8%	50.0%	35.0%	48.4%
	Ours	57.2%	38.0%	54.5%	56.4%	82.5%
	Improvement	+14.4%	+15.9%	+9.0%	+61.1%	+70.5%
Mistral-7B	Baseline	66.0%	21.8%	46.0%	50.0%	50.0%
	Ours	89.0%	54.0%	66.0%	<u>92.1%</u>	61.1%
	Improvement	+34.8%	+147.7%	+43.5%	+84.2%	+22.2%
Claude-3.5	Baseline	98.4%	72.0%	52.0%	50.5%	50.0%
	Ours	100.0%	98.7%	83.0%	86.3%	82.5%
	Improvement	+1.6%	+37.1%	+59.6%	+70.9%	+65.0%
Gemini-pro	Baseline	96.0%	56.7%	49.0%	48.5%	55.9%
	Ours	<u>98.0%</u>	<u>82.8%</u>	<u>73.5%</u>	70.1%	66.2%
	Improvement	+2.1%	+46.0%	+50.0%	+44.5%	+18.4%
GPT-3.5	Baseline	81.0%	40.7%	37.0%	49.5%	50.0%
	Ours	92.1%	55.3%	58.5%	61.5%	<u>92.1%</u>
	Improvement	+13.7%	+35.9%	+58.1%	+24.2%	+84.2%
GPT-4o-mini	Baseline	89.0%	37.3%	44.0%	57.0%	82.3%
	Ours	100.0%	77.8%	68.0%	92.5%	92.7%
	Improvement	+12.4%	+108.6%	+54.5%	+62.3%	+12.6%

Table 2: **Average performance of LLMs on IoT tasks.** **HAR-2cls** stands for classifying walking and standing activities. **HAR-3cls** stands for classifying lying, walking upstairs, and transitioning from lying to sitting activities. **Heartbeat** stands for classifying normal and abnormal heartbeats. **Machine** stands for determining whether the coolers work properly or not. **Occupancy** stands for detecting the presence of a person in a room.

as GPT-4o-mini and Claude-3.5, can effectively perform various IoT-sensory tasks, particularly excelling in HAR using IMU data. However, their performance is limited when faced with more challenging tasks that involve complex data and require specialized knowledge. For example, in heartbeat anomaly detection, LLMs perform sub-optimally due to the time-series nature and numerical complexity of ECG data. Simplifying the data miti-

gates some challenges but does not address the fundamental model limitations. Additionally, LLMs lack the extensive medical knowledge necessary for comprehensive analysis. While retrieved knowledge may suffice for simpler tasks, more complex problems might require further model fine-tuning to incorporate deeper medical expertise.

LLMs are excellent learners in IoT-sensory task reasoning. Without domain-specific knowledge

Method	IoT tasks (Accuracy ↑)				
	HAR-2cls	HAR-3cls	Machine	Heartbeat	Occupancy
Baseline	89.0%	37.3%	57.0%	44.0%	82.3%
+ IoT data simplification and enrichment	92.0%	43.3%	58.3%	53.0%	83.0%
+ retrieved domain knowledge	92.4%	59.3%	66.4%	55.3%	85.3%
+ retrieved demonstrations	99.0%	66.7%	86.4%	64.0%	87.7%
Full setting	100.0%	77.8%	92.5%	68.0%	92.7%

Table 3: Ablation study of different modules within our framework.

and relevant demonstrations, LLMs face significant challenges in performing IoT-sensory tasks, often resorting to near-random guessing, especially in tasks such as heartbeat anomaly detection. This indicates that real-world tasks remain challenging for LLMs to execute directly. However, LLMs are excellent learners, and their capabilities can be significantly enhanced through our proposed framework. Specifically, the LLama2-7B, Mistral-7B, Claude-3.5, Gemini-pro, GPT-3.5, and GPT-4o-mini models exhibit average performance improvements of 30%, 58%, 48%, 41%, 48%, and 49% respectively across various tasks, underscoring the effectiveness of our methodology.

LLMs can address tasks from an expert perspective. Compared with the baseline method, our framework enables LLMs to perform in-depth, targeted data analysis akin to that of a domain expert. While the baseline allows LLMs to provide logically consistent but often superficial analyses based on IoT data—lacking specificity and deep exploration of data characteristics—our framework enhances their capabilities through advanced data and knowledge integration. This results in more comprehensive analyses and professional responses. For example, in heartbeat anomaly detection (see Fig. 3), the baseline method mentions general features like peaks and rhythms but offers only broad descriptions of fluctuations, failing to identify critical abnormalities such as compensatory pauses and waveform irregularities. This leads to vague and incomplete reasoning. In contrast, our method meticulously identifies and examines key features, such as premature ventricular contractions (PVCs) characterized by early ventricular contractions followed by compensatory pauses, which are essential for accurate PVC diagnosis. This comparison demonstrates that by enhancing perceptual and knowledge-based capabilities, our framework significantly improves LLMs’ ability to deeply under-

stand IoT data and its physical context, enabling precise, expert-level analysis.

4.3 Ablation study

To evaluate the impact of different components within our framework, we performed an ablation study using GPT-4o-mini. We tested the following configurations: (1) IoT data simplification and enrichment, (2) addition of retrieved domain knowledge based on (1), (3) inclusion of retrieved demonstrations based on (2), and (4) the full configuration, which incorporates role descriptions and chain-of-thought techniques as outlined in the Prompt Configuration stage. The results, presented in Table 3, reveal that for straightforward tasks such as classifying walking and standing activities, IoT data simplification and enrichment and domain knowledge retrieval are sufficient. However, for more complex tasks, the inclusion of additional modules significantly boosts performance. Overall, our findings indicate that each module in our framework progressively enhances the ability of LLMs to perform IoT-sensory tasks using IoT data.

5 Conclusion

LLMs often face challenges in real-world tasks that require an understanding of physical laws. To address this limitation, we introduce IoT-LLM, a novel framework that integrates IoT sensor data with LLMs to enhance their perception and reasoning capabilities in the physical world. We developed a new benchmark comprising five IoT-sensory tasks, each varying in data types and reasoning complexity, and evaluated six open-source and proprietary LLMs. Our experimental results indicate that IoT-LLM significantly improves the reasoning performance of LLMs on IoT-sensory tasks, with models such as GPT-4o-mini showing an average improvement of 49.4% across various tasks compared to previous methods. This approach sys-

tematically enhances the applicability of LLMs in real-world scenarios by effectively leveraging IoT data.

Limitations

Our work primarily focuses on low-dimensional IoT data, demonstrating that under our proposed framework, LLMs can effectively interpret such low-complexity data to perform real-world tasks. However, we did not conduct experiments on higher-dimensional data. LLMs encounter significant challenges with higher-dimensional data, such as audio and 3D point cloud data, due to their extensive length and complexity. Integrating such data into the context of LLMs is both difficult and impractical. Instead, directly fine-tuning LLMs with data specific to these modalities may be a more effective approach. Future research could explore this strategy to extend the capabilities of LLMs to handle more complex data types within the IoT domain.

References

- Josh Achiam, Steven Adler, Sandhini Agarwal, Lama Ahmad, Ilge Akkaya, Florencia Leoni Aleman, Diogo Almeida, Janko Altenschmidt, Sam Altman, Shyamal Anadkat, and 1 others. 2023. Gpt-4 technical report. *arXiv preprint arXiv:2303.08774*.
- Hussam Alkaissi and Samy I McFarlane. 2023. Artificial hallucinations in chatgpt: implications in scientific writing. *Cureus*, 15(2).
- Andreas Blattmann, Tim Dockhorn, Sumith Kulal, Daniel Mendeleevitch, Maciej Kilian, Dominik Lorenz, Yam Levi, Zion English, Vikram Voleti, Adam Letts, and 1 others. 2023. Stable video diffusion: Scaling latent video diffusion models to large datasets. *arXiv preprint arXiv:2311.15127*.
- Tim Brooks, Bill Peebles, Connor Holmes, Will DePue, Yufei Guo, Li Jing, David Schnurr, Joe Taylor, Troy Luhman, Eric Luhman, Clarence Ng, Ricky Wang, and Aditya Ramesh. 2024. [Video generation models as world simulators](#).
- Tom Brown, Benjamin Mann, Nick Ryder, Melanie Subbiah, Jared D Kaplan, Prafulla Dhariwal, Arvind Neelakantan, Pranav Shyam, Girish Sastry, Amanda Askell, and 1 others. 2020. Language models are few-shot learners. *Advances in neural information processing systems*, 33:1877–1901.
- Patricia S. Churchland and Terrence J. Sejnowski. 1988. [Perspectives on cognitive neuroscience](#). *Science*, 242 4879:741–5.
- Hongwei Cui, Yuyang Du, Qun Yang, Yulin Shao, and Soung Chang Liew. 2023. Llmind: Orchestrating ai and iot with llms for complex task execution. *arXiv preprint arXiv:2312.09007*.
- Anna Dawid and Yann LeCun. 2023. Introduction to latent variable energy-based models: A path towards autonomous machine intelligence. *arXiv preprint arXiv:2306.02572*.
- Alexey Dosovitskiy, Lucas Beyer, Alexander Kolesnikov, Dirk Weissenborn, Xiaohua Zhai, Thomas Unterthiner, Mostafa Dehghani, Matthias Minderer, Georg Heigold, Sylvain Gelly, Jakob Uszkoreit, and Neil Houlsby. 2020. [An image is worth 16x16 words: Transformers for image recognition at scale](#). *ArXiv*, abs/2010.11929.
- Jiachen Du, Boyang Jia, and Xinyi Fu. 2023. Space brain: An ai autonomous spatial decision system. In *CAAI International Conference on Artificial Intelligence*, pages 61–67. Springer.
- Evelina Fedorenko, Steven T Piantadosi, and Edward AF Gibson. 2024. Language is primarily a tool for communication rather than thought. *Nature*, 630(8017):575–586.
- Quentin Garrido, Mahmoud Assran, Nicolas Ballas, Adrien Bardes, Laurent Najman, and Yann LeCun. 2024. Learning and leveraging world models in visual representation learning. *arXiv preprint arXiv:2403.00504*.
- Ary Goldberger, Luís Amaral, L. Glass, Shlomo Havlin, J. Hausdorg, Plamen Ivanov, R. Mark, J. Mietus, G. Moody, Chung-Kang Peng, H. Stanley, and PhysioToolkit Physiobank. 2000. Components of a new research resource for complex physiologic signals. *PhysioNet*, 101.
- Julie Grèzes, Pierre Fonlupt, Bennett I. Bertenthal, Chantal Delon-Martin, Christoph Segebarth, and Jean Decety. 2001. [Does perception of biological motion rely on specific brain regions?](#) *NeuroImage*, 13:775–785.
- Nate Gruver, Marc Finzi, Shikai Qiu, and Andrew G Wilson. 2024. Large language models are zero-shot time series forecasters. *Advances in Neural Information Processing Systems*, 36.
- Nikolai Helwig, Eliseo Pignanelli, and Andreas Schtze. 2018. Condition monitoring of hydraulic systems. UCI Machine Learning Repository. DOI: <https://doi.org/10.24432/C5CW21>.
- Jonathan Ho, Ajay Jain, and P. Abbeel. 2020. [Denosing diffusion probabilistic models](#). *ArXiv*, abs/2006.11239.
- Lucie Hobeika, C. Diard-Detoef, Béatrice Garcin, Richard Levy, and Emmanuelle Volle. 2016. [General and specialized brain correlates for analogical reasoning: A meta-analysis of functional imaging studies](#). *Human Brain Mapping*, 37.

- He Huang, Jianfei Yang, Xu Fang, Hao Jiang, and Lihua Xie. 2022. Varifi: Variational inference for indoor pedestrian localization and tracking using imu and wifi rss. *IEEE Internet of Things Journal*, 10(10):9049–9061.
- Lei Huang, Weijiang Yu, Weitao Ma, Weihong Zhong, Zhangyin Feng, Haotian Wang, Qianglong Chen, Weihua Peng, Xiaocheng Feng, Bing Qin, and 1 others. 2023. A survey on hallucination in large language models: Principles, taxonomy, challenges, and open questions. *arXiv preprint arXiv:2311.05232*.
- Sijie Ji, Xinzhe Zheng, and Chenshu Wu. 2024. Hargpt: Are llms zero-shot human activity recognizers? *arXiv preprint arXiv:2403.02727*.
- Fu Li, Jiaming Huang, Yi Gao, and Wei Dong. 2023. Chatiot: Zero-code generation of trigger-action based iot programs with chatgpt. In *Proceedings of the 7th Asia-Pacific Workshop on Networking*, pages 219–220.
- Hao Liu, Wilson Yan, Matei Zaharia, and Pieter Abbeel. 2024. World model on million-length video and language with ringattention. *arXiv preprint arXiv:2402.08268*.
- Ze Liu, Yutong Lin, Yue Cao, Han Hu, Yixuan Wei, Zheng Zhang, Stephen Lin, and Baining Guo. 2021. Swin transformer: Hierarchical vision transformer using shifted windows. *2021 IEEE/CVF International Conference on Computer Vision (ICCV)*, pages 9992–10002.
- Somayya Madakam, Ramya Ramaswamy, and Sidharth Tripathi. 2015. Internet of things (iot): A literature review. *Journal of Computer and Communications*, 3(5):164–173.
- R OpenAI. 2023. Gpt-4 technical report. arxiv 2303.08774. *View in Article*, 2(5).
- Joon Sung Park, Joseph O’Brien, Carrie Jun Cai, Meredith Ringel Morris, Percy Liang, and Michael S Bernstein. 2023. Generative agents: Interactive simulacra of human behavior. In *Proceedings of the 36th annual acm symposium on user interface software and technology*, pages 1–22.
- William Peebles and Saining Xie. 2023. Scalable diffusion models with transformers. In *Proceedings of the IEEE/CVF International Conference on Computer Vision*, pages 4195–4205.
- Mykhailo Poliakov and Nadiya Shvai. 2024. Multi-meta-rag: Improving rag for multi-hop queries using database filtering with llm-extracted metadata. *ArXiv*, abs/2406.13213.
- Alec Radford, Karthik Narasimhan, Tim Salimans, Ilya Sutskever, and 1 others. 2018. Improving language understanding by generative pre-training.
- Alec Radford, Jeffrey Wu, Rewon Child, David Luan, Dario Amodei, Ilya Sutskever, and 1 others. 2019. Language models are unsupervised multitask learners. *OpenAI blog*, 1(8):9.
- Jorge Reyes-Ortiz, Davide Anguita, Luca Oneto, and Xavier Parra. 2015. Smartphone-based recognition of human activities and postural transitions. UCI Machine Learning Repository. DOI: <https://doi.org/10.24432/C54G7M>.
- Rebecca Saxe, Susan L. Whitfield-Gabrieli, Jonathan Scholz, and Kevin A. Pelphrey. 2009. Brain regions for perceiving and reasoning about other people in school-aged children. *Child development*, 80 4:1197–209.
- Dimitris Spathis and Fahim Kawsar. 2023. The first step is the hardest: Pitfalls of representing and tokenizing temporal data for large language models. *Journal of the American Medical Informatics Association : JAMIA*.
- Jason Wei, Xuezhi Wang, Dale Schuurmans, Maarten Bosma, Ed Huai hsin Chi, F. Xia, Quoc Le, and Denny Zhou. 2022. Chain of thought prompting elicits reasoning in large language models. *ArXiv*, abs/2201.11903.
- Huatao Xu, Liying Han, Qirui Yang, Mo Li, and Mani Srivastava. 2024a. Penetrative ai: Making llms comprehend the physical world. In *Proceedings of the 25th International Workshop on Mobile Computing Systems and Applications*, pages 1–7.
- Huatao Xu, Liying Han, Qirui Yang, Mo Li, and Mani Srivastava. 2024b. Penetrative AI: Making LLMs comprehend the physical world. In *Findings of the Association for Computational Linguistics ACL 2024*, pages 7324–7341, Bangkok, Thailand and virtual meeting. Association for Computational Linguistics.
- Jianfei Yang, He Huang, Yunjiao Zhou, Xinyan Chen, Yuecong Xu, Shenghai Yuan, Han Zou, Chris Xiaoxuan Lu, and Lihua Xie. 2024. Mm-fi: Multi-modal non-intrusive 4d human dataset for versatile wireless sensing. *Advances in Neural Information Processing Systems*, 36.
- Jingyi Zhang, Jiaying Huang, Sheng Jin, and Shijian Lu. 2024a. Vision-language models for vision tasks: A survey. *IEEE Transactions on Pattern Analysis and Machine Intelligence*.
- Xiyuan Zhang, Ranak Roy Chowdhury, Rajesh K. Gupta, and Jingbo Shang. 2024b. Large language models for time series: A survey. *ArXiv*, abs/2402.01801.
- Lexin Zhou, Wout Schellaert, Fernando Martínez-Plumed, Yael Moros-Daval, Cèsar Ferri, and José Hernández-Orallo. 2024. Larger and more instructable language models become less reliable. *Nature*, pages 1–8.

Andrii Zhuravchak, Oleg Kapshii, and Evangelos Pournaras. 2022. Human activity recognition based on wi-fi csi data-a deep neural network approach. *Procedia Computer Science*, 198:59–66.

A Details about IoT-oriented knowledge retrieval augmentation

Construct IoT knowledge base. We firstly construct IoT domain knowledge base and demonstration knowledge base, which will be utilized for retrieving domain knowledge and task-specific demonstrations. For the IoT domain knowledge base, we gather relevant documents (e.g., Wikipedia articles, research papers) through web searches. To ensure comprehensive coverage of IoT data and tasks, we focus on documents encompassing the following themes: (1) IoT data domain knowledge, (2) IoT task domain knowledge, and (3) expert insights on leveraging IoT data for task execution. For instance, in the context of using ECG data to detect abnormal heartbeats, we collect documents that (1) provide detailed explanations of ECG data, such as the significance of various fluctuations, (2) describe the task of heartbeat anomaly detection and the distinctions between normal and abnormal heartbeats, and (3) elucidate the phenomena observed in ECG data when a heartbeat is abnormal. For the demonstration knowledge base, we create task-specific demonstrations authored by human experts or AI models (e.g., ChatGPT). These demonstrations include task description (question), a step-by-step analysis of the task using the provided IoT data (optional), and the final answer to the task.

Embed knowledge base into vector database. After constructing the knowledge bases, we employ an embedding model (e.g., text-embedding-ada-002³ by OpenAI) to transform the knowledge base into vector database. Specifically, we segment documents into smaller chunks (e.g., split by every two sentences). Demonstrations, being shorter in length, are embedded as single chunks. The embedding model then converts these chunks into vector embeddings. Finally, we store these text chunks and corresponding embeddings as key-value pairs, which allows for efficient and scalable search capabilities. To improve the quality of retrieved contents, we also store metadata (e.g. IoT data type for IoT domain knowledge base and task type for

demonstration knowledge base) alongside the vector embeddings within the vector database. This approach allows for advanced post-processing techniques, such as metadata filtering (Poliakov and Shvai, 2024), to refine search results and improve task-specific retrieval accuracy.

IoT-oriented retrieval. In this step, we retrieve relevant knowledge using both IoT data descriptions and task descriptions as query. We employ two types of retrievers for this purpose: (1) sparse keyword-based retrievers and (2) dense embedding-based retrievers. The former identifies similar documents based on shared keywords between the document and the query, excelling in keyword matching but potentially missing semantically similar information. The latter operates at the embedding level, requiring the embedding of IoT data descriptions and task descriptions using the same embedding model as in the previous step to generate query vectors. This kind of retriever is adept at identifying semantically relevant content but may overlook precise interpretations of technical terms. Given that our data descriptions and task descriptions contain numerous numerical data and specialized terminology, we adopt a hybrid search method, which means utilizing both types of retrievers to harness their unique strengths, ensuring the consistent retrieval of highly relevant and context-rich information. Specifically, we retrieve $2n$ pieces of texts using each type of retriever (n pieces per type) and then apply a re-ranking technique to recalibrate the similarity between the query and documents using ranker models (e.g. bge-reranker-base⁴), filtering out the top- m most relevant pieces. Ultimately, this process yields pertinent knowledge, encompassing documents with specific domain knowledge and task demonstrations relevant to the task at hand.

It is important to note that we don't need to construct each knowledge base for each task especially, instead, we just need to construct two knowledge bases in total (i.e., one IoT domain knowledge base and one demonstration knowledge base), each of which contains all the domain/demonstration knowledge about the total five tasks. During the retrieval phase, we can easily fetch pertinent knowledge precisely corresponding to the task utilizing metadata (e.g., IoT data type and task type) stored within the bases. For demonstrations, we utilize the one-shot setting, which means we retrieve one

³<https://platform.openai.com/docs/guides/embeddings>

⁴<https://huggingface.co/BAAI/bge-reranker-base>

example for each category in classification tasks.

B Details about Datasets used in experiments

Human Activity Recognition. We employ the Smartphone-Based Recognition of Human Activities and Postural Transitions Dataset (Reyes-Ortiz et al., 2015). This dataset comprises raw IMU data, specifically 3-axial linear acceleration, and 3-axial angular velocity, captured at a sampling rate of 50Hz by the smartphone’s accelerometer and gyroscope. The data encompasses twelve distinct activities. To reduce both the sequence length and data complexity, we down-sample the data to 10Hz. Given the challenges associated with multi-class classification for LLM, instead of utilizing all twelve activity categories, we conduct a binary classification task involving the WALKING and STANDING labels, and a ternary classification task with the LYING, WALKING UPSTAIRS, and LIE TO SIT labels. We evaluate the average correction performance using 100 samples per label.

Industrial anomaly detection. We employ the Condition Monitoring of Hydraulic Systems Dataset (Helwig et al., 2018), which facilitates the assessment of a hydraulic test rig’s condition using multi-sensor data, including temperature, cooling power, and efficiency factor series, all experimentally derived from the rig. The dataset categorizes cooler conditions into three severity grades: (1) close to failure; (2) reduced efficiency; and (3) full efficiency. For simplicity, we focus on a binary classification task using only “close to failure” and “full efficiency” categories. We evaluate the average correction performance using 700 samples per label.

Heartbeat anomaly detection. We employ the MIT-BIH Arrhythmia Database (Goldberger et al., 2000). This dataset comprises ECG recordings from 48 subjects, each sampled at 360Hz, and categorizes heartbeats into several types, including Normal beat (N), Atrial premature beat (A), and Premature ventricular contraction (V), among others. To reduce the difficulty of the task, we down-sample the signals to 72Hz and focus on a binary classification task using only the Normal beat (N) and Premature ventricular contraction (V) categories. We evaluate the average correction performance using 500 samples per category.

Human sensing task. We utilize a dataset collected using a TP-Link TL-WDR4300 WiFi router operating at 5 GHz with a 40 MHz bandwidth (Zhuravchak et al., 2022). The dataset specifically captures the absence of human presence across three different rooms. Each room’s environment is carefully monitored to record Channel State Information (CSI) that reflects the presence or absence of occupants, providing a robust basis for occupancy detection tasks. For the experiment, we evaluate the average correction performance using 500 samples per category.

Indoor localization task. We utilize a dataset collected in a laboratory environment using an IoT system developed in (Huang et al., 2022). The dataset consists of RSSI signals, the basis for determining human positions within the space. By collecting RSS fingerprints at various reference points, a signal radio map is constructed using a modified Gaussian Process Regression (GPR) method. This approach allows us to estimate the RSS distribution at any given location, providing a reliable means of localizing human presence in the environment. A total of 2,000 samples were utilized to compute the evaluation metrics mentioned in the experiment.

C Experimental Cost

Unlike related works such as Penetrative AI and HarGPT, the expert knowledge utilized in our experiments does not require manual, task-specific design. Instead, relevant domain-specific articles are collected from online resources or literature to construct a knowledge base, with task-specific expert knowledge automatically retrieved as needed. Consequently, the experimental cost in this study is primarily limited to the API usage fees for closed-source models.

For open-source LLMs such as LLama2-7B, inference was conducted locally, utilizing an A6000 GPU equipped with 48GB of VRAM. In contrast, for closed-source models like GPT-4o-mini, gemini-pro, and claude, inference was performed via their respective official APIs, where costs are determined by the number of tokens processed. In our experiments, the average inference cost per 100 samples was \$0.26 for GPT-3.5-turbo, \$0.10 for GPT-4o-mini, \$1.00 for gemini-pro, and \$2.50 for claude-3.5-sonnet. Based on the total number of samples processed, the overall API expenditure amounted to approximately \$450.

D Prompt and Response examples of LLMs for IoT-sensory tasks

In the Prompt Configuration stage of our framework, we systematically organize IoT data descriptions, task descriptions, relevant knowledge (encompassing IoT domain expertise and task-specific demonstrations), and role descriptions to construct the final prompt according to a predefined template, as illustrated in Fig. 4. For instance, using this template, we derive the final prompt for heartbeat anomaly detection, depicted in Fig. 5.

We present examples of responses generated by LLMs across all five applications mentioned in our work, including human activity recognition, industrial anomaly detection, heartbeat anomaly detection, WiFi-based human sensing, and indoor localization, as illustrated in Fig. 7, Fig. 8, Fig. 9, Fig. 10, and Fig. 11. To emphasize the LLM outputs, we provide only the raw IoT sensor data and corresponding user queries, excluding detailed prompts.

{Role definition}

The combined application of these knowledge and skills would enable you to accurately perform the task and provide relevant analysis and interpretation

EXPERT:

{Retrieved domain knowledge}

EXAMPLES:

{Retrieved task-specific demonstrations}

THE GIVEN DATA:

{IoT data description}

QUESTION:

{Task description}

Please analyze the data step by step to explain what it reflects, and then provide your answer based on your analysis.

ANALYSIS:

ANSWER:

Figure 4: Final prompt template.

You are an experienced physician who is familiar with various types of electrocardiogram (ECG) data. You can easily make preliminary judgments on whether heartbeats are abnormal based on ECG data. You possess the following medical and domain knowledge:

1. ECG Interpretation: You understand the basic principles of electrocardiography and know how to interpret ECG waveforms, including identifying different phases of the cardiac cycle and recognizing abnormalities.
2. Cardiac Physiology: You are familiar with the physiological functions of the heart, the generation and propagation of cardiac electrical signals, and the characteristics and manifestations of various cardiac arrhythmias.
3. Recognition of ECG Abnormalities: You are able to identify abnormal waveforms in ECG data, such as arrhythmias, myocardial ischemia, myocardial infarction, etc., and differentiate them from normal ECG patterns.
4. Medical Statistics: You are proficient in statistical analysis of ECG data, identification of outliers, and quantitative assessment of abnormalities.
5. Clinical Experience: You have extensive clinical experience to integrate ECG data with patient symptoms and medical history for accurate diagnosis and evaluation.
6. Medical Ethics and Legal Knowledge: You understand medical ethics and legal regulations to ensure confidentiality and lawful use of patient data.

The combined application of these domain knowledge and skills would enable you to accurately assess whether there are any abnormalities in the ECG data and provide relevant analysis and interpretation.

EXPERT:

Electrocardiography is the process of producing an electrocardiogram (ECG or EKG[a]), a recording of the heart's electrical activity through repeated cardiac cycles.[4] It is an electrogram of the heart which is a graph of voltage versus time of the electrical activity of the heart[5] using electrodes placed on the skin. In clinical applications, labeled ECG data are used to build a heartbeat classification system. Then this system is used to determine the types of heartbeats in unknown patients' ECG recordings. The overall magnitude of the heart's electrical potential is then measured from twelve different angles ("leads") and is recorded over a period of time (usually ten seconds). In this way, the overall magnitude and direction of the heart's electrical depolarization is captured at each moment throughout the cardiac cycle. A premature heart beat or extrasystole[1] is a heart rhythm disorder corresponding to a premature contraction of one of the chambers of the heart. Premature heart beats come in two different types: premature atrial contractions and premature ventricular contractions. Diagnosis Normal sinus rhythm and ectopic beats - premature ventricular contractions (PVC) and premature atrial contractions (PAC) shown on an EKG PVCs may be found incidentally on cardiac tests such as a 12-lead electrocardiogram (ECG/EKG) performed for another reason. In those with symptoms suggestive of premature ventricular complexes, the ECG/EKG is the first investigation that may identify PVCs as well as other cardiac rhythm issues that may cause similar symptoms. You can analyze whether the heartbeat is normal by considering a combination of factors such as the amplitude of peaks or valleys appearing in the electrocardiogram (ECG) time series, the time intervals between adjacent peaks or valleys, and the fluctuations in voltage values within the ECG data.

EXAMPLE1:

THE GIVEN ECG DATA:

-0.39mV, -0.38mV, -0.36mV, -0.355mV, -0.35mV, -0.37mV, -0.365mV, -0.35mV, -0.335mV, -0.35mV, -0.345mV, -0.355mV, -0.35mV, -0.33mV, -0.32mV, -0.295mV, -0.29mV, -0.295mV, -0.285mV, -0.23mV, -0.165mV, -0.08mV, -0.03mV, -0.1mV, -0.15mV, -0.185mV, -0.185mV, -0.16mV, -0.095mV, 0.325mV, 1.02mV, 0.53mV, -0.15mV, -0.22mV, -0.26mV, -0.305mV, -0.335mV, -0.31mV, -0.295mV, -0.275mV, -0.27mV, -0.245mV, -0.21mV, -0.145mV, -0.09mV, -0.03mV, 0.04mV, 0.105mV, 0.23mV, 0.365mV, 0.475mV, 0.52mV, 0.48mV, 0.375mV, 0.275mV, 0.16mV, 0.075mV, 0.0mV, -0.08mV, -0.135mV

ANSWER: Normal heartbeat (N)

EXAMPLE2:

THE GIVEN ECG DATA:

-0.55mV, -0.41mV, -0.29mV, -0.24mV, -0.16mV, -0.105mV, -0.08mV, -0.04mV, -0.055mV, -0.005mV, 0.085mV, 0.21mV, 0.42mV, 0.63mV, 0.785mV, 0.875mV, 0.9mV, 0.83mV, 0.705mV, 0.56mV, 0.405mV, 0.21mV, 0.125mV, 0.12mV, 0.08mV, 0.065mV, 0.06mV, 0.18mV, 0.48mV, 1.05mV, 1.57mV, 1.25mV, 0.81mV, 0.9mV, 0.05mV, -0.365mV, -0.525mV, -0.69mV, -0.76mV, -0.62mV, -0.79mV, -0.68mV, -0.685mV, -0.735mV, -0.785mV, -0.795mV, -0.82mV, -0.775mV, -0.7mV, -0.6mV, -0.485mV, -0.355mV, -0.24mV, -0.14mV, -0.115mV, -0.11mV, -0.115mV, -0.11mV, -0.085mV, -0.095mV

ANSWER: Premature ventricular contraction (V)

THE GIVEN DATA:

-0.205mV, -0.195mV, -0.155mV, -0.05mV, -0.015mV, 0.02mV, 0.125mV, 0.21mV, 0.345mV, 0.47mV, 0.615mV, 0.675mV, 0.705mV, 0.655mV, 0.6mV, 0.47mV, 0.36mV, 0.2mV, 0.135mV, 0.095mV, 0.045mV, 0.09mV, 0.025mV, 0.055mV, 0.05mV, 0.065mV, 0.14mV, 0.27mV, 0.29mV, 0.825mV, 1.35mV, 0.655mV, -1.18mV, -0.96mV, -0.89mV, -0.67mV, -0.47mV, -0.335mV, -0.27mV, -0.145mV, -0.12mV, -0.08mV, -0.1mV, -0.07mV, -0.005mV, 0.055mV, 0.155mV, 0.31mV, 0.52mV, 0.705mV, 0.875mV, 0.92mV, 0.865mV, 0.75mV, 0.6mV, 0.44mV, 0.245mV, 0.19mV, 0.125mV, 0.055mV

The ECG data is collected from a patient's heart. The data consists of a series of electrical signals that represent the heart's electrical activity. The signals are measured in millivolts (mV) and are recorded over a period of time at the sampling frequency of 60Hz. This means there is an interval of 0.017 seconds between the two voltage values. The data is divided into two categories: normal heartbeats (N) and ventricular ectopic beats (V). The normal heartbeats represent the regular electrical activity of the heart, while the ventricular ectopic beats represent abnormal electrical activity. The data is collected using a single-channel ECG device.

QUESTION:

Is the ECG heartbeat signal normal or abnormal?

Please analyze the data step by step to explain what it reflects, and then provide your answer based on your analysis.

ANALYSIS:

ANSWER:

Figure 5: Final prompt for heartbeat anomaly detection. Note that role description is generated automatically by AI models (e.g., ChatGPT).

1. (Triaxial acceleration signal) :

X-axis: 1.361 , 1.328 , 1.316 , 1.414 , 1.452 , 1.247 , 0.893 , 0.58 , 0.527 , 0.858 , 1.053 , 1.09 , 0.971 , 0.873 , 0.909 , 0.623 , 0.793 , 0.951 , 0.861 , 0.986 , 0.889 , 0.874 , 0.89 , 1.091 , 1.0 , 0.984 , 0.986 , 0.99 , 1.289 , 1.022 , 1.049 , 1.118 , 1.228 , 1.046 , 1.192 , 0.947 , 0.77 , 0.861 , 1.057 , 1.236 , 1.245 , 1.16 , 1.001 , 1.008 , 0.746 , 0.961 , 0.868 , 0.666 , 0.593 , 0.788 , 0.637 , 0.653 , 0.754 , 1.313 , 0.832 , 0.833 , 0.965 , 1.124 , 1.269 , 1.573 , 1.38 , 1.226 , 1.356 , 1.049 , 1.373 , 1.067 , 0.55 , 0.542 , 0.915 , 0.749 , 0.99 , 0.925 , 0.841 , 0.825 , 0.77 , 0.728 , 0.751 , 0.834 , 0.984 , 1.002 , 1.133 , 0.921 , 0.92 , 0.952 , 0.951 , 1.43 , 0.983 , 1.001 , 1.076 , 1.137 , 1.036 , 1.258 , 1.184 , 1.07 , 0.88 , 0.789 , 0.798 , 1.289 , 1.396 , 1.249 , 0.788 , 0.932 , 0.893 , 0.909 , 0.844 , 1.013 , 0.758 , 0.742 , 0.687 , 0.678 , 1.425 , 0.773 , 0.821 , 0.855 , 0.952 , 0.881 , 1.236 , 1.336 , 1.336 , 1.342 , 0.916 , 1.472 , 1.421 , 1.108 , 0.63 , 0.529 , 0.837 , 0.826

Y-axis: ...

Z-axis:...

2. (Triaxial angular velocity signal) :

X-axis: -0.015, -0.317, -0.377, -0.268, 0.15, 0.883, 0.61, 0.07, -0.403, -0.8, -0.923, -0.661, -0.013, 0.323, 0.47, 0.446, 0.133, 0.238, 0.214, 0.262, 0.044, 0.017, 0.031, 0.072, 0.157, 0.588, 0.476, 0.509, 0.456, 0.292, 0.036, -0.009, 0.056, -0.075, -0.665, 0.39, -1.524, -0.833, 0.059, 0.743, -0.033, 0.305, -0.154, -0.562, -0.673, -0.374, -0.397, -0.352, -0.151, -0.082, -0.385, 0.199, 0.141, 0.261, 0.147, -0.182, -0.111, -0.378, -0.408, -0.401, 0.302, -0.505, -0.434, -0.018, 0.58, -0.717, 0.534, 0.145, -0.469, -1.032, 0.181, -0.559, -0.105, 0.37, 0.416, 0.498, 0.344, 0.424, 0.404, 0.261, 0.16, 0.124, 0.087, 0.21, 0.318, 0.371, 0.353, -0.957, 0.078, 0.101, 0.187, 0.113, 0.909, -1.101, -1.475, -1.093, -0.524, 0.16, -0.582, 0.467, 0.145, -0.085, -0.5, -0.243, -0.659, -0.794, -0.549, -0.435, 0.161, 0.009, 0.067, 0.18, 0.071, -0.084, -0.151, -0.0, -0.109, -0.049, -0.13, -0.289, -0.443, -0.452, 0.593, 0.798, -0.089, 0.074, -0.52, 0.922

Y-axis: ...

Z-axis: ...



1. Triaxial acceleration signal:

X-axis: 1.3 6 1 g, 1.4 5 2 g, 0.8 5 8 g, 0.9 0 9 g, 0.8 6 1 g, 1.0 9 1 g, 1.2 8 9 g, 1.0 4 6 g, 1.0 5 7 g, 0.7 4 6 g, 0.7 8 8 g, 1.3 1 3 g, 1.2 9 6 g, 1.0 4 9 g, 0.7 7 9 g, 1.1 3 3 g, 1.4 3 g, 1.0 3 6 g, 0.7 9 8 g, 0.7 8 8 g, 1.0 1 3 g, 1.4 2 5 g, 0.8 8 1 g, 0.9 1 6 g, 0.8 2 6 g

Y-axis: ...

Z-axis: ...

X-axis-mean=1.0 3 4 g, X-axis-var=0.0 5 3

Y-axis-mean=-0.1 6 9 g, Y-axis-var=0.0 3 2

Z-axis-mean=-0.0 0 7 g, Z-axis-var=0.0 4 7

2. Triaxial angular velocity signal:

X-axis: -0.0 1 5 rad/s, 0.8 8 3 rad/s, -0.6 6 1 rad/s, 0.1 3 3 rad/s, 0.2 6 2 rad/s, 0.5 8 8 rad/s, 0.0 3 6 rad/s, 0.3 9 rad/s, -0.0 3 3 rad/s, -0.3 7 4 rad/s, -0.3 8 5 rad/s, -0.1 8 2 rad/s, 0.3 0 2 rad/s, -0.7 1 7 rad/s, 0.1 8 1 rad/s, 0.3 4 4 rad/s, 0.1 2 4 rad/s, -0.9 5 7 rad/s, 0.9 0 9 rad/s, -0.5 8 2 rad/s, -0.2 4 3 rad/s, 0.1 6 1 rad/s, -0.0 rad/s, -0.4 5 2 rad/s, -0.0 8 9 rad/s, 0.9 2 2 rad/s

Y-axis: ...

Z-axis: ...

X-axis-mean=0.0 2 1 rad/s, X-axis-var=0.2 3 5

Y-axis-mean=0.1 3 8 rad/s, Y-axis-var=0.5 0 7

Z-axis-mean=-0.0 2 6 rad/s, Z-axis-var=0.0 6 5

1. Triaxial acceleration signal:
The provided three-axis acceleration signals contain acceleration data for the X-axis, Y-axis, and Z-axis respectively. Each axis's data is a time-series signal consisting of some data samples, measured at a fixed time interval with a frequency of 10Hz(10 samples is collected per second) by smartphone (Samsung Galaxy S II) wearing on the waist. The unit is gravitational acceleration (g), equivalent to 9.8m/s². It's important to note that the measured acceleration is influenced by gravity, meaning the acceleration measurement along a certain axis will be affected by the vertical downward force of gravity.

2. Triaxial angular velocity signal:
The provided three-axis angular velocity signals contain angular velocity data for the X-axis, Y-axis, and Z-axis respectively. Each axis's data is a time-series signal consisting of some data samples, measured at a fixed time interval with a frequency of 10Hz. The unit is radians per second (rad/s).

Figure 6: During IoT data simplification and enrichment stage, raw IoT data is transformed into IoT data description, which is easier to understand by LLMs. Raw IoT data is enriched with descriptive metadata, including natural language expressions of implicit physical information like units. Specialized tokenization techniques and extraction of temporal or frequency domain features further enhance LLMs’ understanding of numerical and time-series data. These improvements make IoT data more accessible and interpretable for LLMs, facilitating its use in real-world applications.

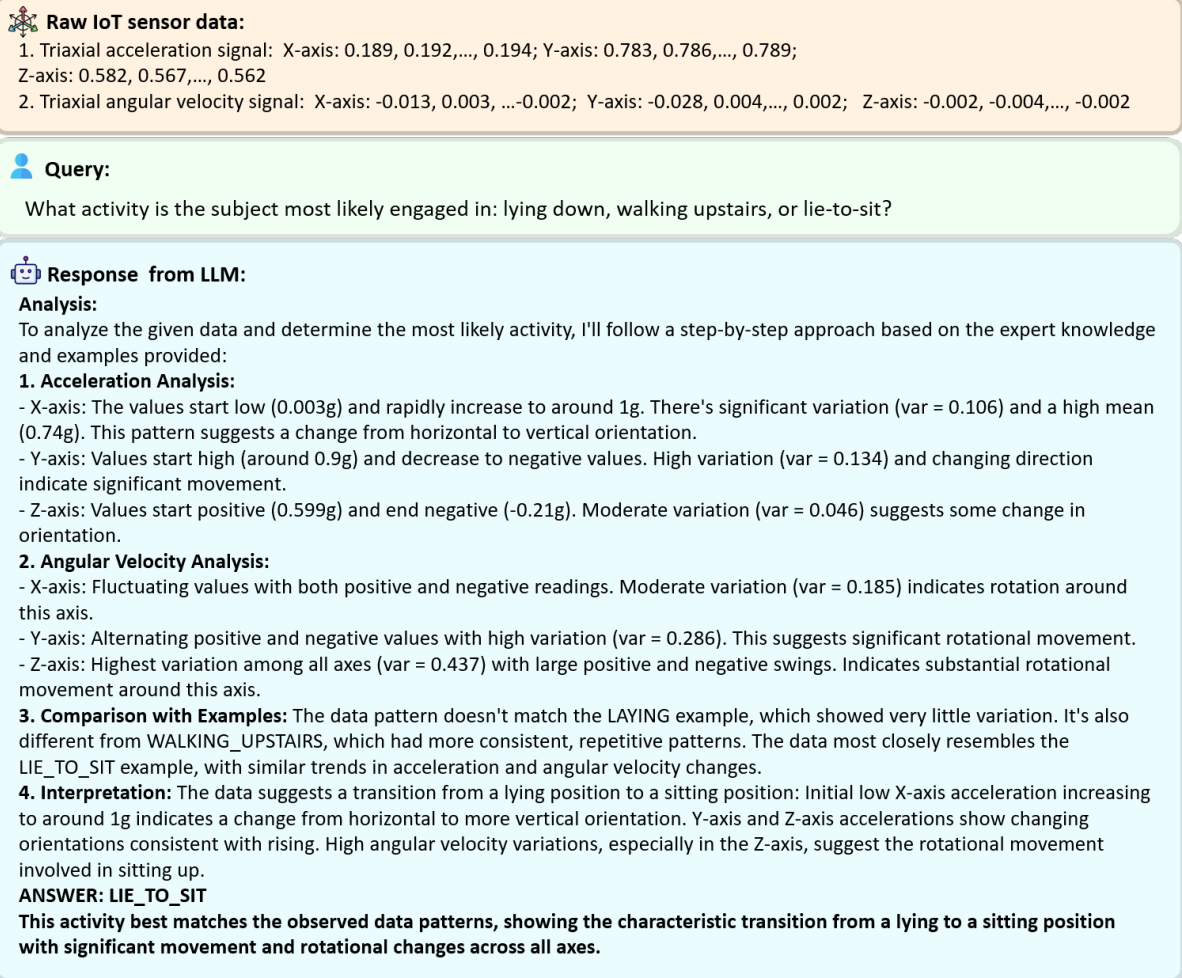


Figure 7: Response example of LLM for human activity recognition.



Raw IoT sensor data:

1. Temperature Change Sequence: 57.277, ..., 57.301
2. Cooling Power Change Sequence: 1.488, 1.497, ..., 1.495
3. Cooling Efficiency Change Sequence: 18.704, ..., 18.821



Query

Is the machine's cooling system functioning properly?



Response from LLM:

To analyze the operational status of the machine's cooling system, we'll examine the Temperature Change Sequence, Cooling Power Change Sequence, and Cooling Efficiency Change Sequence step by step.

1. Temperature Change Sequence Analysis:

The sequence starts at 55.836°C and fluctuates throughout the 60-second period, with a slight increasing trend towards the end, closing at 55.75°C. The temperature shows a range of fluctuations but remains within a relatively narrow band (~55.5°C to ~56.0°C). This indicates that while there is a slight increase, the temperature does not significantly spike or drop, suggesting a potentially stable but slightly elevated operational temperature.

2. Cooling Power Change Sequence Analysis:

The cooling power starts at 1.568KW and shows variability throughout the sequence, peaking at 1.636KW and then decreasing towards the end, closing at 1.568KW. The cooling power's fluctuations are relatively minor, indicating that the cooling system is adjusting its output in response to the system's needs. However, the fact that it increases and then returns to the starting value suggests that the cooling system is actively working to manage the temperature, albeit with varying degrees of success.

3. Cooling Efficiency Change Sequence Analysis:

The cooling efficiency begins at 20.09% and exhibits some variability, peaking at 20.908% and then showing a decrease in efficiency towards the end, closing at 20.125%. The efficiency values indicate that the cooling system's effectiveness in removing heat from the system varies but reaches relatively high efficiency levels during the sequence. The decrease towards the end suggests a reduction in cooling performance over time.

Final Analysis and Conclusion:


The data reflects a cooling system that is actively working to manage the machine's temperature, as evidenced by the fluctuations in cooling power and efficiency. However, several indicators suggest that the cooling system may not be functioning optimally:

- The temperature, while relatively stable, is on the higher side throughout the sequence and shows a slight increasing trend. This suggests that the cooling system might be struggling to maintain or lower the temperature effectively.
- The cooling power shows that the system is adjusting its output, but the return to the initial value suggests that these adjustments may not be fully effective over time.
- The cooling efficiency, despite reaching relatively high levels, decreases towards the end of the sequence, indicating a potential drop in the cooling system's performance.

Based on this analysis, while the cooling system is operational and making adjustments in response to the machine's cooling needs, the slight increase in temperature, along with the variability in cooling power and the drop in efficiency towards the end, suggests that the cooling system may not be functioning at its best. It appears to be underperforming, possibly due to issues like partial blockages, reduced coolant flow, or other inefficiencies within the system.

ANSWER: The machine's cooling system is not functioning properly and may require maintenance or further inspection to address potential issues affecting its performance.

Figure 8: Response example of LLM for industrial anomaly detection.

 **Raw IoT sensor data:**

-0.205, -0.195, -0.155, -0.05, -0.015, 0.02, 0.125, 0.21, , ..., 0.055

 **Query:**

Is it a Normal heartbeat(N) or Premature ventricular contraction beat(V)?

 **Response from LLM:**

To analyze the given ECG data, we will follow a systematic approach, examining the amplitude, intervals, and progression of the electrical signal that represents a heartbeat. This will involve looking for patterns that match either a normal heartbeat or a premature ventricular contraction (PVC).

Step 1: Baseline and P-wave Identification

- The initial segment shows a gradual increase in amplitude from -0.22mV to 0.125mV, which could represent the P-wave and the beginning of the QRS complex. In a normal heartbeat, the P-wave represents atrial depolarization. The gradual increase is consistent with the expected pattern, although the amplitude is somewhat low for a typical P-wave, which might not be clearly defined in this case.

Step 2: QRS Complex Analysis

- The amplitude sharply rises to 1.15mV, which is a characteristic feature of the QRS complex, representing ventricular depolarization. This sharp rise is expected in both normal and PVC beats. However, the amplitude of 1.15mV is within a normal range for the QRS complex, not indicating an overtly abnormal morphology based on amplitude alone.

Step 3: Examination of the ST Segment and T-wave

- After the peak, there's a dramatic drop to -1.395mV, which is highly unusual for a normal T-wave following the QRS complex. In a normal ECG, the T-wave represents ventricular repolarization and should be a positive deflection following the QRS complex, not a sharp negative drop. This significant negative deflection is not characteristic of a normal T-wave and indicates a significant abnormality.

Step 4: Checking for Premature Beat

- The dramatic changes in amplitude, especially the sharp drop after the peak, could suggest a PVC. PVCs are characterized by an abnormal QRS complex, which is wide and has an unusual shape. The drop to -1.395mV could be interpreted as part of an abnormally wide and bizarre QRS complex, which is a hallmark of PVCs. However, the presence of a preceding P-wave-like activity and the recovery back towards a more normal rhythm pattern complicate the interpretation slightly.

Step 5: Final Analysis and Conclusion

- The data shows a significant deviation from the normal ECG pattern, especially with the dramatic drop after the peak, which is not characteristic of a normal T-wave. The overall pattern suggests a significant abnormality in the ventricular repolarization process. Given the sharp rise indicative of the QRS complex followed by an abnormal repolarization phase, the pattern is more suggestive of a PVC due to the abnormal and dramatic changes in voltage that do not follow the typical progression of a normal heartbeat.

ANSWER: Premature ventricular contraction beat (V)

This conclusion is based on the abnormal morphology of the waveform, particularly the unusual negative deflection following what appears to be the QRS complex, which does not align with the expected pattern of a normal T-wave. This analysis highlights the importance of examining the entire ECG waveform, including the amplitude, intervals, and progression of electrical activity, to differentiate between normal heartbeats and arrhythmias such as PVCs.

Figure 9: Response example of LLM for heartbeat anomaly detection.



Raw IoT sensor data:

```
[[0.12233546, 0.23833588, 0.21289147, 0.200783 , 0.35365783, 0.29699911, 0.19572163, ..., 0.21170883],  
 [0.11896763, 0.23593459, 0.21084769, 0.19843066, 0.31336457, 0.29052874, ..., 0.25554572, 0.24116531],  
 ...]
```



Query:

Is there is a person or not?



Response from LLM:

To determine whether there is a person present based on the given data, we will analyze the provided values against the characteristics of the "no_person" and "have_person" classes.

Given Data:

1. **Mean value of CSI:** 0.282172876639514852.
2. **Standard deviation across subcarriers for the mean CSI amplitude over time:** 0.015816562357126943.
3. **Mean standard deviation across subcarriers for each time point:** 0.04446593535538511

Reference Values:

1. No_person:

Mean value of CSI: 0.29408252935437873 (larger than have_person)

Standard deviation across subcarriers for the mean CSI amplitude over time: 0.01709716445812625 (smaller than have_person)

Mean standard deviation across subcarriers for each time point: 0.03370765374037318 (smaller than have_person)

2. Have_person:

Mean value of CSI: 0.272173948247671 (smaller than no_person)

Standard deviation across subcarriers for the mean CSI amplitude over time: 0.022446105102973825 (larger than no_person)

Mean standard deviation across subcarriers for each time point: 0.051079445194106045 (larger than no_person)

Step-by-Step Analysis:

1. **Mean value of CSI:** The given mean value (0.28217287663951485) is between the mean values of "no_person" (0.29408252935437873) and "have_person" (0.272173948247671). This suggests a possibility of human presence, as it is closer to the "have_person" mean.
2. **Standard deviation across subcarriers for the mean CSI amplitude over time:** The given standard deviation (0.01581656235712694) is smaller than the "no_person" standard deviation (0.01709716445812625) and also smaller than the "have_person" standard deviation (0.022446105102973825). This indicates that the variability is not increased, which is contrary to the expected behavior if a person were present.
3. **Mean standard deviation across subcarriers for each time point:** The given mean standard deviation (0.04446593535538511) is larger than the "no_person" mean standard deviation (0.03370765374037318) but smaller than the "have_person" mean standard deviation (0.051079445194106045). This suggests some degree of variability, but it does not exceed the threshold expected for a "have_person" scenario.

Conclusion:

The analysis indicates that while the mean value of CSI is closer to the "have_person" category, the standard deviation across subcarriers for the mean CSI amplitude over time is lower than expected for a "have_person" scenario. Moreover, the mean standard deviation across subcarriers for each time point is not sufficiently high to classify it as "have_person." Given these observations, the data suggests that the environment is more likely consistent with the "no_person" category.

ANSWER: no_person

Figure 10: Response example of LLM for WiFi-based human sensing.



Raw IoT sensor data:

[-120.0, 0.0], [-64, -44, -54, -64, -68, -53]



Query:

Based on the given data, estimate the x-y position.



Response from LLM:

To estimate the x-y position using the WKNN algorithm based on the provided RSSI sample and the top-3 neighbors, we will follow these steps:

1. Input Data:

RSSI Sample: [-64, -44, -54, -64, -68, -53]

Top-3 Neighbors' Positions: [[-1880, 0], [-1880, 0], [-1880, 0]]

Corresponding Similarities: [0.70710678, 0.37796447, 0.18569534]

2. Compute Sum of Similarities:

We first compute the sum of the similarities of the top-3 neighbors.

$$\sum_{similarity} = 0.70710678 + 0.37796447 + 0.18569534 = 1.27076659$$

3. Compute Weights for Each Neighbor:

The weights for each neighbor are calculated by normalizing the similarities.

$$Weights = \frac{Similarities}{\sum_{similarity}} = \frac{0.70710678 \quad 0.37796447 \quad 0.18569534}{1.27076659 \quad 1.27076659 \quad 1.27076659}$$

Which gives: $Weights \approx 0.55636853, 0.29757729, 0.14605418$.

4. Estimate Position Using Weighted Average:

Now we will calculate the estimated position using the weighted average of the neighbors' positions.

$$estimated\ position = \sum weights \times neighbor\ positions$$

$$Breaking\ this\ down:\ estimated\ position = [0.55636853 \times -1880 + 0.29757729 \times -1880 + 0.14605418 \times -1880, \quad 0.55636853 \times 0 + 0.29757729 \times 0 + 0.14605418 \times 0] = [(-1880) \times (0.55636853 + 0.29757729 + 0.14605418), 0] = [(-1880) \times 1.00000000, 0] = [-1880, 0]$$

5. Final Answer: The estimated location based on the analysis is:

ANSWER = "[-1880, 0]"

Thus, the estimated location is "[-1880, 0]".

Figure 11: Response example of LLM for WiFi-based indoor localization.